RAPID COMMUNICATIONS

PHYSICAL REVIEW B VOLUME 52, NUMBER 20 15 NOVEMBER 1995-II

Mechanisms of initial alloy formation for Pd on Cu(100) studied by STM

P. W. Murray, I. Stensgaard, E. Lægsgaard, and F. Besenbacher

Center for Atomic-Scale Materials Physics, and Institute of Physics and Astronomy, University of Aarhus, DK 8000 Aarhus C, Denmark

(Received 27 June 1995; revised manuscript received 11 August 1995)

The nucleation and growth of Pd alloys on Cu(100), up to the ordered $c(2\times2)$ structure have been studied using scanning tunneling microscopy. Atomically resolved images at low Pd coverages (0.20 ML) show protrusions, located in the lattice sites of the substrate, that are attributed to individual Pd atoms. A pair-correlation plot shows that there is a strong tendency for them to be located in second-nearest-neighbor positions, resulting in the formation of short chains along the [001] and [010] directions. As the coverage increases, the chains converge to form a $c(2\times2)$ structure, with the squeezed-out Cu atoms nucleating into Cu islands. The Cu islands also form over the alloyed regions, with the result that more than the previously reported 0.5 ML of Pd is required to form the $c(2\times2)$ structure with second-layer growth initiated before a perfect $c(2\times2)$ structure is formed.

Over the past few years there has been considerable interest in the study of metal on metal growth from both a fundamental point of view and the technological relevance of novel chemical, electronic, and magnetic properties of thin films. In many cases, surface alloys are formed in which the deposited metal intermixes with the topmost layer of the substrate rather than forming a simple overlayer structure, and such alloys have even been observed between metals which are immiscible in the bulk.[1] Information regarding the intermixing and alloy formation is important in understanding the properties of such structures. However, for a number of systems, little detailed information regarding the initial stages of alloy formation at the atomic level is available. For Cu(100), a number of metal adsorbates, such as Au,[2] Mn,[3–5] and Pd,[6–9] are known to form a surface alloy with a $c(2\times2)$ structure at a coverage of approximately 0.5 ML. In these studies only the $c(2\times2)$ structure has been investigated. Even in the case of STM studies on Au (Ref. 2) and Mn (Refs. 4 and 5) alloying, no detailed information was obtained on the nucleation and growth of $c(2\times2)$ alloys on Cu(100).

Due to its relevance as a bimetallic catalyst, for example in methanol synthesis, where it is believed to show superior reactivity and selectivity properties,[10] Pd alloying on Cu(100) has been the subject of a number of investigations. Low-energy electron diffraction (LEED) studies of Pd deposition on Cu(100) (Ref. 9) have reported a $c(2\times2)$ structure and ruled out the formation of an ordered $c(2\times2)$ overlayer in favor of a surface alloy. The alloyed Pd atoms were relaxed 0.02 Å outwards from the Cu atoms and the interlayer spacing of the first layer with regard to the second was close to that of pure Cu, with photoemission results[9] showing the appearance of Pd features similar to those seen for Cu-rich bulk CuPd alloys. Local-density approximation (LDA) calculations[11] also support the surface alloy model in favor of an ordered Pd overlayer. However, the coverage required for an ordered $c(2\times2)$ structure is still a matter of debate, with Graham and co-workers[8,12] reporting the optimal coverage of 0.8 ML while Pope, Griffiths, and Norton[6] and Wu *et al.*[9] reported that 0.55 ML was the best coverage. Low-energy ion scattering (LEIS) studies[12] have suggested that Pd is located subsurface due to the Cu signal only decaying to 70% upon formation of the $c(2\times2)$ structure compared to the expected 50%. More recently, Valden *et al.*[13] reported that by using CO as a probe molecule for a Pd coverage of 0.5 ML, approximately 40% of the outer layer was pure Cu, with the remaining Pd located below the surface.

In this paper we show in detail, using STM, how the initial nucleation and growth of a $c(2\times2)$ alloy occurs on the Cu(100) surface upon Pd deposition. Furthermore, the mechanism for incorporation of subsurface Pd is revealed and an explanation is provided for the reported discrepancy in the coverage required to form a well-ordered $c(2\times2)$ phase. At low coverages a pair-correlation plot of the Pd atom positions shows a preference for the Pd atoms to occupy second-nearest-neighbor (NN) positions, resulting in the formation of rows along the [010] or [001] directions. Correlated with the formation of the rows we observe the formation of Cu islands. Alloy formation is also observed on the islands although the Pd density is somewhat less than on the terraces, indicating that Pd atoms beneath the islands remain subsurface. Upon increased Pd coverage the Pd chains converge into structures with a local $c(2\times2)$ periodicity. Due to the incorporation of Pd below the surface layer, significantly more Pd is required to form large $c(2\times2)$ domains than the ideal 0.5 ML. Finally, the nucleation of a second-layer structure is observed before completion of the $c(2\times2)$ structure, which, together with the presence of subsurface Pd, explains the discrepancy in the coverages previously reported for the $c(2\times2)$ phase.

These experiments were performed using a fully automated STM (Ref. 14) operated at room temperature (RT). The STM was mounted in an ultrahigh vacuum (UHV) chamber, interfaced to a 2-MV Van de Graaff accelerator via differential pumping, and containing standard facilities for sample cleaning and characterization. The Cu(100) crystal was prepared by repeated cycles of Ne ion bombardment (3 keV) and annealing (770 K) until judged clean and ordered by Auger electron spectroscopy (AES), LEED, and STM. Pd evaporation was carried out by resistively heating a conical tungsten filament which contained a Pd wire, and the absolute Pd coverage calibrations were obtained by Rutherford

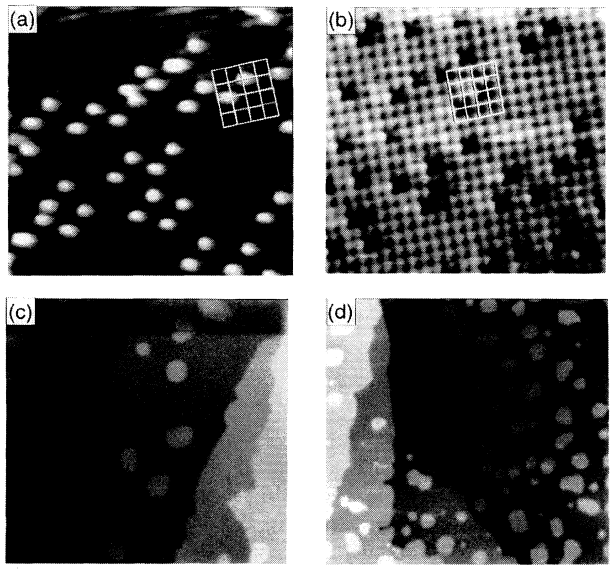

FIG. 1. (a) 50×50-Å^2 image of Cu(100) after 0.20-ML Pd deposition, showing the appearance of protrusions on the substrate upon which a (1×1) unit mesh is superimposed. (b) After a tip change the protrusions can be imaged as depressions (50×50 Å^2). (c) 1000×1000-Å^2 image after 0.20-ML Pd deposition showing the formation of islands on the terraces, and a roughening of step edges. (d) 1500×1500-Å^2 image after 0.40-ML Pd deposition showing the nucleation of smaller islands in between the larger ones.

backscattering spectroscopy (RBS).[15] Pd deposition was carried out with the sample at RT with the source being allowed to stabilize before exposure of the sample. STM images were recorded in the constant current mode with typical tunneling parameters of 2 nA current and −10 mV sample bias. Changes in polarity had no significant effect on the images.

Figure 1(a) shows an STM image recorded after deposition of 0.20 ML as determined by RBS. A number of small protrusions can be observed on the image, and by superimposing a (1×1) unit mesh on the image it can be concluded that the protrusions are located directly on Cu sites in the surface. The height of these features varies from 0.1 to 0.3 Å, depending on such factors as tunneling parameters and tip quality. Occasionally after a tip change they can be imaged as depressions as illustrated in Fig. 1(b), indicating that the contrast is strongly dependent on the chemical identity of the tip. During repeated scans over the same area, no evidence was observed for any diffusion of the protrusions, indicating their stability in the Cu substrate. Increasing the Pd exposure results in an increase in the number of protrusions. Correlated with the formation of protrusions we observe the formation of islands on the terraces as shown in Fig. 1(c), the heights of which are consistent with a monatomic step on Cu(100). Atomically resolved images of such islands show that the atomic structure is consistent with a Cu(100)1×1 surface and thus we attribute the protrusions to Pd atoms alloyed into the surface layer and the islands to Cu atoms ejected from the terraces by surface alloy formation. A similar interpretation was given for Au alloying on Ni(110).[1] Pd atoms are also observed on the islands, although their density is somewhat less than on the terraces, especially at the edges of the islands. As the Pd coverage increases, so does the area covered by the islands, as evidenced in Fig. 1(d). However, in regions with a high step density, very few islands are seen, suggesting that the ejected Cu atoms diffuse to nearby step edges. This is further supported by the observation that the step edges are more jagged as compared to the smooth step edges on clean Cu(100). Similar observations have been made for steps on Cu(100) surfaces alloyed with Mn and Au, which results in Cu islands or expanding step edges.[2,4]

Returning to the density of Pd atoms on the terrace, the coverage determined from a number of STM images, similar to Fig. 1(a), is 0.15 ML, somewhat less than that obtained from RBS (0.20 ML). However, RBS is not as surface sensitive as STM and therefore any Pd located below the first layer would be detected by RBS. Previous studies of the $c(2\times2)$ alloy structure have indicated that some Pd is located subsurface.[12,13] Given that the density of Pd on islands and close to step edges is less than that on the terraces, this would indicate that Pd located below the islands does not diffuse to the surface. Thus we ascribe the discrepancy between the STM and RBS coverage determinations to Pd located under newly formed islands and expanding step edges. A one-to-one correspondence between the deposited Pd and ejected Cu atoms is difficult to determine experimentally, due to the fact that it is impossible to identify the amount of Cu that has migrated to steps.

We now focus on the distribution of the Pd atoms on the terraces. From the images of Fig. 1(a) the majority of Pd atoms appear to be located in a second NN position to another Pd atom, that is preferentially aligned along the [010] and [001] directions. This is quantified further in Fig. 2(a), which shows a pair-correlation plot of the NN distribution for Pd atoms out to a distance of sixth NN positions taken over a number of images with a Pd coverage of 0.20 ML (RBS). Also shown for comparison are the expected occupations based on a perfect random distribution, and a simulation generated for the number of images and Pd atoms used in the data set. The latter gives a measure of the reliability of the data set; the more closely this matches the distribution of random positions, the more statistically reliable is the data set. It can be seen from the histogram that the distribution is not random, with very few Pd atoms located in first NN sites, while there is a significant increase in the occupation of second NN positions, that is, along the [010] and [001] directions. This is consistent with recent calculations on surface alloying by Tersoff,[16] which take into account the strain energy caused by atomic size mismatch. These have shown that a second NN occupancy is energetically favorable for alloying on metal (100) surfaces. Thus, the initial stages of alloy formation proceed via the formation of chains along the [001] and [010] directions with an elongation of the chains as the coverage increases. The formation of longer chains is seen in Fig. 2(b), where the Pd coverage is increased to 0.35 ML, as determined by RBS. Where the chains converge, small $c(2\times2)$ units are formed. The discrepancy between the coverage determined from a number of STM images (0.29 ML) and RBS (0.35 ML) is again attributed to subsurface Pd. Examination of the Cu island size and distribution reveals that at low Pd coverages islands are formed at typical separations of 150 to 200 Å, indicating that the diffusion length of the Cu atoms on the alloyed surface is on the order

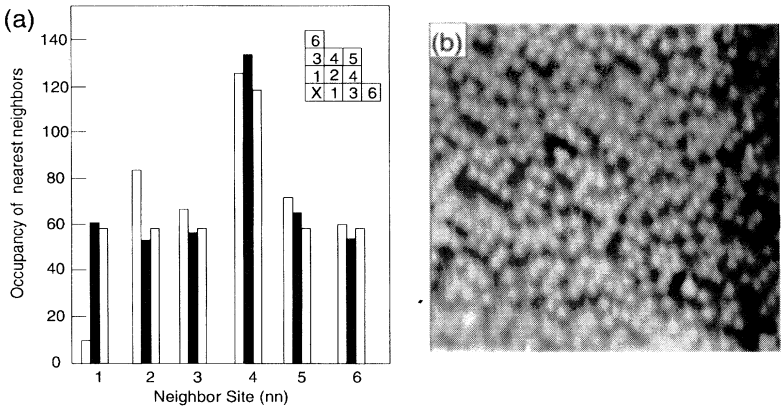

FIG. 2. (a) Histogram of the occupancy of Pd atoms as a function of NN distance up to sixth NN for 96 Pd atoms from a number of images at 0.20-ML coverage (open bars), the expected occupancy for a totally random distribution (shaded bars), and a random simulation on the images the data was acquired from (filled bars). There are significantly smaller (greater peaks) for the first (second) NN positions. (b) 100×100-Å^2 image at 0.45-ML Pd, revealing the formation of short rows of Pd atoms along the [001] and [010] directions. Where the chains converge small $c(2\times2)$ domains are formed.

of 100 Å. Further deposition causes the islands to increase in size. However, as the Pd coverage increases beyond 0.4 ML, the island sizes remain constant and new smaller islands are formed in the areas between the larger islands and also closer to the step edges. This can be interpreted as an indication of a reduction in the mobility of the Cu atoms as the Pd coverage increases, with the density of Pd chains at low coverages being insufficient to make any noticeable difference to the mobility so that the islands increase in size. As the chain density increases, it impedes the diffusion of Cu atoms, resulting in the nucleation of new islands.

Figure 3 shows an STM image recorded after increasing the Pd coverage to 0.55 ML (RBS), in order to try to achieve a sufficient density of chains to create large ordered domains of the $c(2\times2)$. Such domains are indeed observed, but they show a high density of defects (13%). Corrugation heights within the $c(2\times2)$ structure are measured to be on the order of 0.15 Å, compared to the 0.02-Å displacement obtained from LEED data.[9] STM studies on Cu(100)$c(2\times2)$Au alloyed surfaces[2] indicate a similar corrugation despite the greater mismatch in size for Au, again indicating that the corrugation measurements are dependent on the electronic as well as the geometric structure of the surface. It can also be seen that in the vicinity of the upper step edges there is a significantly reduced concentration of Pd. This further substantiates the assumption that Cu, ejected by the formation of the alloy, migrates to step edges, in addition to the formation of islands, with the alloy on the lower terrace extending right up to the step. Furthermore, there do not appear to be any domain boundaries within the $c(2\times2)$ structure, despite the initial nucleation of the Cu-Pd rows being independent. This suggests that as the coverage increases and the chains converge to form small domains, there is movement of the Pd chains as the $c(2\times2)$ structures are formed so as to align

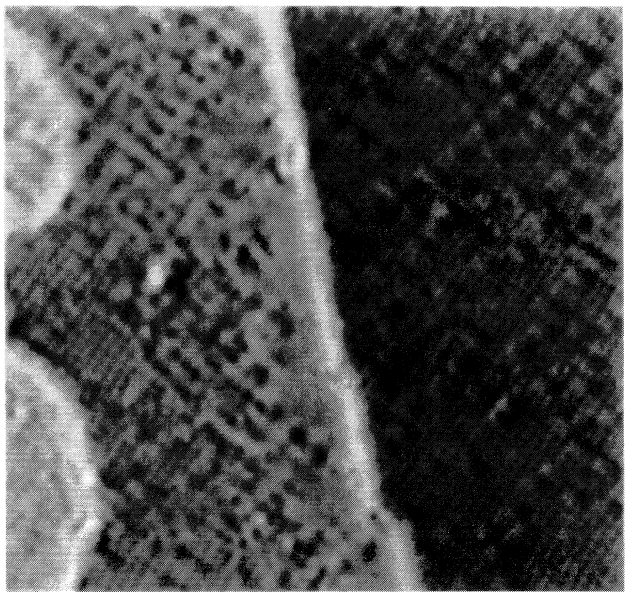

FIG. 3. 200×200-Å^2 STM image following 0.55-ML Pd deposition. Domains of $c(2\times2)$ structures can be seen although there is a high density of defects (13%). Note the lack of Pd features on the upper step edge in the center of the image.

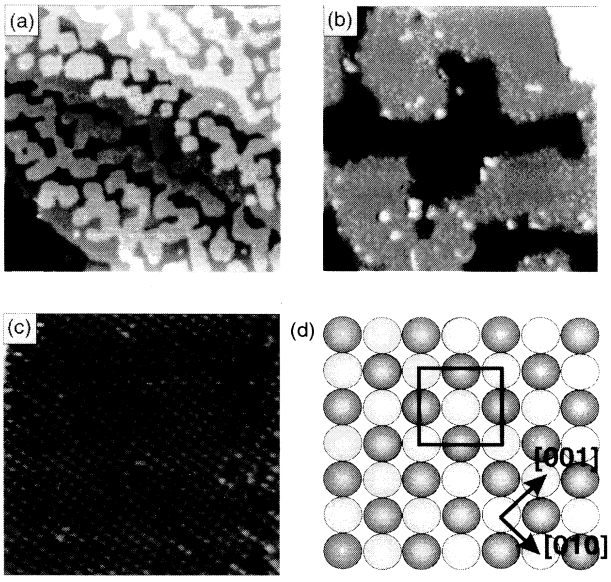

FIG. 4. (a) 1500×1500-Å^2 image following 1.10-ML Pd deposition, showing the merging of islands and steps. (b) 300×300-Å^2 image showing the nucleation of a second-layer structure at upper step edges. (c) 100×100-Å^2 image recorded away from the step edges showing well-ordered $c(2\times2)$ structures. (d) Schematic model of the $c(2\times2)$ alloy structure. Pd (Cu) atoms are heavily (lightly) shaded circles.

domain walls, which results in large domains.

Only by increasing the coverage well beyond 0.55 ML do we find evidence for well-ordered domains of $c(2\times2)$ structure. Large area images, Fig. 4(a), reveal that the steps and islands have begun to merge, and higher resolution images [Fig. 4(b)] show that on the upper edges of steps and islands the nucleation of a second-layer structure is seen which will be discussed elsewhere,[17] and it is only away from these areas that the well-ordered $c(2\times2)$ phase is observed, as shown in Fig. 4(c). No evidence is seen in the images for any distortion of the $c(2\times2)$ structure due to strain induced by the size mismatch between Pd and Cu, unlike the $c(2\times2)$ alloy structure formed by Au deposition on Cu(100) in which ridges are seen. These results also provide an explanation regarding the variations in coverage required for the $c(2\times2)$ alloy. In most cases, this has been determined by monitoring the intensity of fractional order spots in LEED patterns. By using RBS, Pope *et al.*[7] reported that this corresponded to a coverage of 0.55 ML. Although well-ordered domains are observed away from the step/island edges at these coverages, the LEED pattern is obtained from a much wider area, and consequently will be affected to some extent by the disorder caused to the $c(2\times2)$ structure by growth of the second layer, which nucleates before the $c(2\times2)$ structure is complete. On the other hand, if one reduces the coverage to below the point where second-layer nucleation occurs, then the disorder within the $c(2\times2)$ phase itself increases (Fig. 3), and in areas close to island and step edges there are hardly any ordered Pd features. Thus the two types of disorder will be present over a range of coverages, making it difficult to determine an optimum coverage for a well-ordered $c(2\times2)$ structure.

In summary, we have used STM to show how the initial stages of Pd alloy formation on Cu(100) occur and subsequently results in the formation of an ordered $c(2\times2)$ alloy structure. Atomic resolution images have shown that growth proceeds via the formation of chains along the [010] and [001] directions, with the Pd atoms preferentially occupying second NN positions. Islands of Cu formed by the ejected Cu atoms are also observed, and as the coverage increases the mobility of the Cu atoms is lowered, manifested by the nucleation of new islands in areas between existing ones. Furthermore, the islands are observed to nucleate on top of alloyed areas, thereby resulting in subsurface Pd. The $c(2\times2)$ structure develops as the chains converge, although the long-range order of the $c(2\times2)$ structure is determined by an interplay between defects within the $c(2\times2)$ at lower coverages and the initiation of second-layer growth at increased coverages before the $c(2\times2)$ is fully completed. This provides an explanation for the reported discrepancy in the coverage required to form a well-ordered $c(2\times2)$ structure.

We would like to acknowledge financial support from an EU network on "Bond Making and Breaking at Surfaces," and the Danish Science Research Councils via the "Center for Surface Reactivity," and via the "Center for Atomic-scale Materials Physics" (CAMP), sponsored by the Danish National Research Foundation.

[1] L. Pleth Nielsen, F. Besenbacher, I. Stensgaard, and E. Lægsgaard, Phys. Rev. Lett. **71**, 754 (1993).
[2] D.D. Chambliss and S. Chiang, Surf. Sci. Lett. **264**, L187 (1992).
[3] M. Wuttig, Y. Gauthier, and S. Blugel, Phys. Rev. Lett. **70**, 3619 (1993).
[4] H.P. Noh, T. Hashizume, D. Jeon, Y. Kuk, H.W. Pickering, and T. Sakurai, Phys. Rev. B **50**, 2735 (1994).
[5] R.G.P. van der Kraan and H. van Kempen, Surf. Sci. **338**, 19 (1995).
[6] T.D. Pope, K. Griffiths, and P.R. Norton, Surf. Sci. **306**, 294 (1994).
[7] T.D. Pope, G.W. Anderson, K. Griffiths, P.R. Norton, and G.W. Graham, Phys. Rev. B **44**, 11 518 (1991).
[8] G.W. Graham, P.J. Schmitz, and P.A. Thiel, Phys. Rev. B **41**, 3353 (1990).
[9] S.C. Wu, S.H. Lu, Z.Q. Wang, C.K.C. Lok, J. Quinn, Y.S. Li, D. Tian, F. Jona, and P.M. Marcus, Phys. Rev. B **38**, 5363 (1988).
[10] V. Ponec, Surf. Sci. **272**, 111 (1992).
[11] J. Kudrnovsky, S.K. Bose, and V. Drchal, Phys. Rev. Lett. **69**, 308 (1992).
[12] G.W. Graham, Surf. Sci. **171**, L432 (1986).
[13] M. Valden, J. Aaltonen, M. Pessa, M. Gleeson, and C.J. Barnes, Chem. Phys. Lett. **228**, 519 (1994).
[14] L. Eierdal, F. Besenbacher, E. Lægsgaard, and I. Stensgaard, Surf. Sci. **312**, 31 (1994). The microscope is the prototype of RASTERSCOPE 3000 from DME, Herlev, Denmark.
[15] I. Stensgaard, Rep. Prog. Phys. **55**, 989 (1992).
[16] J. Tersoff, Phys. Rev. Lett. **74**, 424 (1995).
[17] P.W. Murray, I. Stensgaard, E. Lægsgaard, and F. Besenbacher (unpublished).

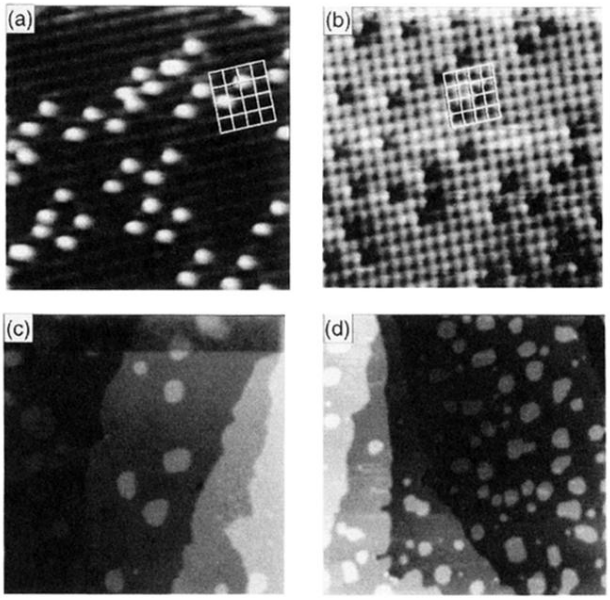

FIG. 1. (a) 50×50-Å^2 image of Cu(100) after 0.20-ML Pd deposition, showing the appearance of protrusions on the substrate upon which a (1×1) unit mesh is superimposed. (b) After a tip change the protrusions can be imaged as depressions (50×50 Å^2). (c) 1000×1000-Å^2 image after 0.20-ML Pd deposition showing the formation of islands on the terraces, and a roughening of step edges. (d) 1500×1500-Å^2 image after 0.40-ML Pd deposition showing the nucleation of smaller islands in between the larger ones.

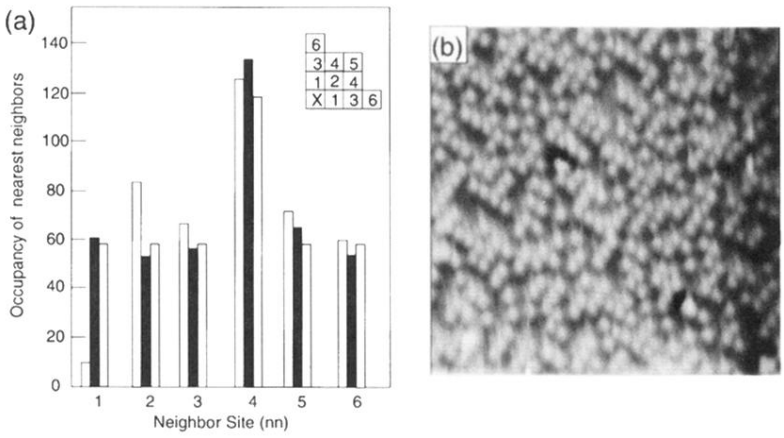

FIG. 2. (a) Histogram of the occupancy of Pd atoms as a function of NN distance up to sixth NN for 96 Pd atoms from a number of images at 0.20-ML coverage (open bars), the expected occupancy for a totally random distribution (shaded bars), and a random simulation on the images the data was acquired from (filled bars). There are significantly smaller (greater peaks) for the first (second) NN positions. (b) 100×100-Å^2 image at 0.45-ML Pd, revealing the formation of short rows of Pd atoms along the [001] and [010] directions. Where the chains converge small $c(2\times2)$ domains are formed.

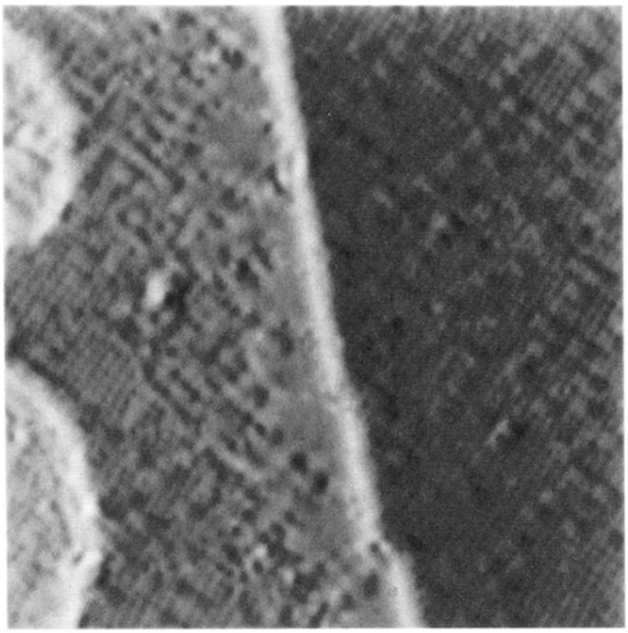

FIG. 3. 200×200-Å^2 STM image following 0.55-ML Pd deposition. Domains of $c(2\times2)$ structures can be seen although there is a high density of defects (13%). Note the lack of Pd features on the upper step edge in the center of the image.

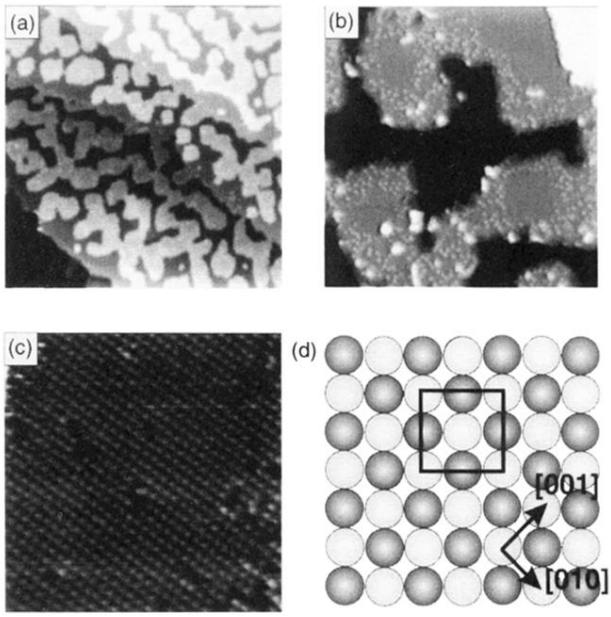

FIG. 4. (a) 1500×1500-Å^2 image following 1.10-ML Pd deposition, showing the merging of islands and steps. (b) 300×300-Å^2 image showing the nucleation of a second-layer structure at upper step edges. (c) 100×100-Å^2 image recorded away from the step edges showing well-ordered $c(2\times2)$ structures. (d) Schematic model of the $c(2\times2)$ alloy structure. Pd (Cu) atoms are heavily (lightly) shaded circles.